Reactions of dinuclear and polynuclear complexes XVI. Chemistry of hydrido-, thiolato-bridged complexes [Mo₂Cp₂(μ-H)(μ-SR)(CO)₄] (R = Me, Ph): Reactivity and electrochemical behaviour; crystal structure of [Mo₂Cp₂(μ-SPh){μ-σ: η²-C(CH₃)=CHCH₃}(CO)₂] [1]

Philippe Schollhammer [a], Francois Y. Pétillon [a,*], Sylvie Poder-Guillou [a], Jean Talarmin [a], Kenneth W. Muir [b,*], Dmitri S. Yufit [b]

[a] *Unité de Recherche associée au CNRS 322, Chimie, Electrochimie Moléculaires et Chimie Analytique, Faculté des Sciences, Université de Bretagne Occidentale, BP 809, 29285 Brest Cédex, France*
[b] *Department of Chemistry, University of Glasgow, Glasgow G12 8Q, UK*

Abstract

Photolysis of [Cp₂Mo₂(μ-H)(μ-ER)(CO)₄] (ER = SMe (**1**) or SPh (**2**)) with MeC≡CMe gives the μ-vinyl complex [Cp₂Mo₂{μ-σ : η²-C(CH₃)=CHCH₃}(μ-ER)(CO)₂] (ER = SMe (**5**) or SPh (**6**)) as the major product. Partial oxidation of **5** leads to the oxo compound [Cp₂Mo₂(O) {μ-σ : η²-C(CH₃)=CHCH₃}(μ-SR)(CO)] (**7**) with a low yield. Compound **6** has been structurally characterized by X-ray diffraction. The structure contains μ-σ : η²-C(CH₃)=CHCH₃ bridging an Mo=Mo double bond whose length is 2.644(1) Å. Chemical deprotonation of [Cp₂Mo₂(μ-H)(μ-ER)(CO)₄] (**1** or **2**) affords the anionic complex [Cp₂Mo₂(μ-ER)(CO)₄]⁻ (R = SMe (**8**) and SPh (**9**)), which is also obtainable by electrochemical reduction. The fluxional behaviour of **8** and **9** and the mechanism of reduction of **1-4** (ER = SᵗBu(**3**) or SePh(**4**)) are described.

1. Introduction

Mononuclear and polynuclear transition metal hydride complexes are of continuing interest because of their key role both in synthesis and catalysis [2]. Compounds containing an {M₂(μ-H)(μ-X)} core are of special importance because the dinuclear framework is maintained by the M₂(μ-X) bridge when organic or inorganic substrates insert into the metal–hydrogen bond. This approach has been extensively developed by Mays and coworkers in their studies of phosphido-bridged manganese [3], molybdenum [4] and other homodimetallic or heterodimetallic complexes [5].

Recently we synthesized the dinuclear (hydrido) thiolato-bridged compounds [Mo₂Cp₂(μ-H)(μ-SR)(CO)₄]

which display fluxionality due to a *cis–trans* interconversion [6]. Their phosphido analogues studied by other groups [4b,7] exhibit very different behaviour related to an equilibrium between two *trans* isomers. The contrast between the properties of the thiolato and phosphido complexes has led us to explore further the chemistry of the (hydrido) thiolato compounds [Mo₂Cp₂(μ-H)(μ-SR)(CO)₄] (R = Me(**1**) or Ph (**2**)).

Among their reactions, insertion of alkyne into the metal–hydrogen bond is one of the most important because it is a key step in catalytic processes involving hydrogenation and polymerization [8,9]. Moreover, this is a convenient way to prepare σ–π alkenyl complexes [4a,10,11]. Very recently, Morris and coworkers [12] reported the synthesis of the dimetallic thiolate complex [Cp₂Mo₂{μ-C(CO₂Me)=CHCO₂Me}(μ-SR)(CO)₂], which has a bridging σ–π alkenyl, by the reaction of the alkyne-bridged species [Cp₂Mo₂(CO)₄{μ-C₂(CO₂Me)₂}] with RSH (R = Et or ᶦPr) [12]. However, the

* Corresponding author.
[1] For Part XV, see [1].

σ–π alkenyl in this complex is stabilized by coordination of the CO_2Me group at its β-carbon atom to one of the molybdenum atoms. No alkenyl compound was obtained when the dimethylacetylenedicarboxylate in the starting complex was replaced by alkynes, such as 2-butyne [12]. Here we show that the μ-vinyl complexes $[Cp_2Mo_2\{\mu\text{-}\sigma : \eta^2\text{-}C(CH_3)=CHCH_3\}(\mu\text{-}SR)(CO)_2]$ (R = Me(5) or Ph(6)) can be obtained by reaction of the (hydrido)thiolato compounds $[Cp_2Mo_2(\mu\text{-}H)(\mu\text{-}SR)(CO)_4]$ (R = Me(1) or Ph(2)) with 2-butyne. In addition, some other aspects of the reactivity of these (hydrido)thiolato complexes are reported and the electrochemical behaviour of $[Cp_2Mo_2(\mu\text{-}H)(\mu\text{-}SR)(CO)_4]$ species (R = Me(1), Ph(2), S^tBu(3) or SePh (4)) examined.

2. Results and discussion

2.1. Reactions of $[Cp_2Mo_2(\mu\text{-}H)(\mu\text{-}SR)(CO)_4]$ (R = Me(1) or Ph (2)) with but-2-yne

2.1.1. Reactions and spectroscopic characterization

Photolysis of $[Cp_2Mo_2(\mu\text{-}H)(\mu\text{-}SR)(CO)_4]$ (R = Me(1) or Ph (2)) in the presence of but-2-yne gives the air-sensitive μ-vinyl complexes $[Cp_2Mo_2\{\mu\text{-}\sigma : \eta^2\text{-}C(CH_3)=CHCH_3\}(\mu\text{-}SR)(CO)_2]$ (R = Me(5) or Ph (6)):

R = Me 1, Ph 2

R = Me 5
R = Ph 6
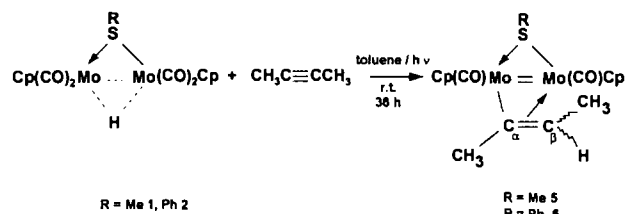
These compounds have been characterized by spectroscopic analyses (Table 1). The IR spectra of 5 and 6 show two weak bands in the ν(CO) region. ^{1}H NMR spectra display a quartet at 6.34 ppm and a doublet at 1.73 ppm $(^3J_{HH}$ gem = 6 Hz), confirming that the alkyne has inserted into the Mo–H bond [4a]. The ^{13}C NMR patterns are consistent with a $\mu\text{-}\sigma : \eta^2$ vinyl structure. The ^{13}C chemical shifts for the σ-bonded (Cα) and the non-σ-bonded (Cβ) C atoms of the μ-vinyl appear at about 184–187 and at 86–88 ppm respectively which accords with a Cα carbene-like character and a Cβ sp^3-like character [10,13]. Two

Table 1
Spectroscopic data of 5–7

Complex	IR [a,b], ν (cm^{-1})	^{1}H NMR [c], δ (ppm)	^{13}C NMR [d], δ (ppm)
5 [a]	1890 (w), 1790 (w)	6.34 (q, 1H, Mo–C(CH$_3$)C(CH$_3$)H, J_{H-H} = 6 Hz), 5.37 (s, 5H, C$_5$H$_5$), 5.18 (s, 5H, C$_5$H$_5$), 2.31 (s, 3H, SCH$_3$), 2.27 (s, 3H, Mo–C(CH$_3$)C(CH$_3$)H), 1.73 (d, 3H, Mo–C(CH$_3$)C(CH$_3$)H, J_{H-H} = 6 Hz)	251.82, 251.62 (CO), 184.72 (Mo–C=C), 92.04, 91.43 (C$_5$H$_5$), 87.82 (Mo–C=C), 33.22, 20.74 (CH$_3$–C=CHCH$_3$), 32.62 (S–CH$_3$)
6 [a]	1900 (w), 1800 (w)	7.32–7.16 (m, 5H, S–C$_6$H$_5$), 6.34 (q, 1H, C=C(CH$_3$)H, J_{H-H} = 6 Hz), 5.42 (s, 5H; C$_5$H$_5$), 5.19 (s, 5H, C$_5$H$_5$), 2.3 (s, 3H, –C(CH$_3$)C=C(CH$_3$)H), 1.72 (d, 3H, –C(CH$_3$)C=C(CH$_3$)H, J_{H-H} = 6 Hz)	250.99, 249.82 (CO), 187.43 (Mo–C=C), 147.85, 130.62, 128.11, 124.86 (S–C$_6$H$_5$), 92.43, 91.90 (C$_5$H$_5$), 86.70 (Mo–C=C), 33.15, 20.78 (CH$_3$–C=CHCH$_3$)
7a [b,e] (54%)	1840 (w), 905 (m)	5.49 (s, 5H, C$_5$H$_5$), 5.02 (s, 5H, C$_5$H$_5$), 3.04 (s, 3H, Mo–C(CH$_3$)C(CH$_3$)H), 3.03 (q, 1H, C=C(CH$_3$)H, J_{H-H} = 6 Hz), 2.40 (s, 3H, SCH$_3$), 1.70 (d, 3H, –C=C(CH$_3$)H, J_{H-H} = 6 Hz)	
7b [c] (46%)		5.41 (s, 5H, C$_5$H$_5$), 5.07 (s, 5H, C$_5$H$_5$), 3.23 (s, 3H, Mo–C(CH$_3$)C(CH$_3$)H), 2.54 (q, 1H, C=C(CH$_3$)H, J_{H-H} = 6 Hz), 2.52 (s, 3H, SCH$_3$), 1.64 (d, 3H, –C=C(CH$_3$)H, J_{H-H} = 6 Hz)	

[a] In CH_2Cl_2 solution.
[b] In KBr pellets.
[c] Measured in $CDCl_3$ at 293 K.
[d] Hydrogen-1 decoupled.
[e] Relative percentages of 7a and 7b given in parentheses.

inequivalent CO and Cp are observed at about 250 and 92 ppm respectively. Elemental analyses are consistent with the proposed stoichiometry for **5** and **6**, but spectroscopic data do not allow either the relative disposition in solution of the Cp and CO ligands or the configuration of the methyl groups in the vinyl ligand (*cis* or *trans*) to be ascertained. A single isomer with inequivalent cyclopentadienyl rings is observed in solution at 293 K. Variable-temperature ^{1}H NMR experiments (between 193 and 293 K) show that the line shapes are not temperature dependent, implying that **5** and **6** are not fluxional.

In addition to **5**, a purple complex resulting from its partial oxidation was isolated with a low yield and identified as a mixture of two isomers which were not separable by column chromatography. They were formulated as the oxo products $[Cp_2Mo_2(O)\{\mu\text{-}\sigma:\eta^2\text{-}C(CH_3)=CHCH_3\}(\mu\text{-}SR)(CO)]$(**7**). The two isomers have similar ^{1}H NMR patterns, which indicates that they have two inequivalent cyclopentadienyl rings, one SMe bridge and a $CH_3C=CHCH_3$ group (Table 1). Their IR spectra show one peak in the $\nu(CO)$ region at 1840 cm^{-1} and another at 905 cm^{-1} attributable to an Mo=O vibration. As was the case for **5** and **6**, the IR and NMR spectra of **7** allow neither the disposition of the cyclopentadienyl rings relative to the Mo–Mo axis nor that of the methyl groups relative the $C\alpha$–$C\beta$ bond to be determined.

Attempts were made to extend this reaction to other symmetrical and unsymmetrical alkynes ($(MeO_2C)CC(CO_2Me)$, PhCCPh, MeCCH, PhCCH and CF_3CCH) but no consistent photochemical insertion occurred, and no product was characterized. This lack of reactivity of the thiolato complexes seems very surprising considering how easily some of the same alkynes insert into Mo–H bond of the analogous phosphido-bridged compounds [4a]. Presumably the phosphido bridge is more effective in stabilizing polynuclear species. This is consistent with the observation that the thiolate group is unable to prevent the break up of the dinuclear framework when attempts were made to insert either alkenes [14] or isocyanide into the M–H bonds of **1** or **2**. Thus the photolytic reaction led to the mononuclear products $[CpMo(CO)(R'NC)_2SR]$ (R' = [1]Bu or xylyl; R = Me or Ph) [15] when RNC was used.

2.1.2. Mechanism of formation of 5–7.

Two alternative pathways for the reaction of alkynes with $[Mn_2(CO)_8(\mu\text{-}H)(\mu\text{-}PPh_2)]$ have been proposed by Mays and coworkers [3c]. One involves initial loss of a CO to give an unsaturated intermediate which can react with the alkyne. The other requires first the coordination of the alkyne concomitantly with the breaking of the metal–metal bond, then the loss of a CO, and finally the insertion of the alkyne in the metal–hydrogen bond. Similar mechanisms may be suggested for the initial
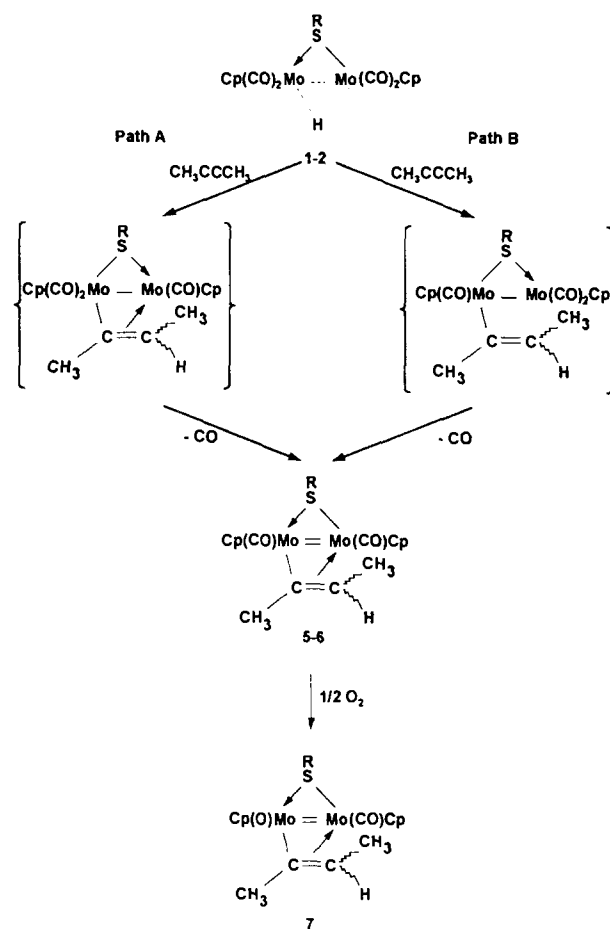
Scheme 1. Proposed mechanism of formation of **5** and **6**.

steps in the formation of the $\mu\text{-}\sigma:\eta^2$ vinyl products. However, the final phosphide and thiolato products, $[Cp_2Mo_2\{\mu\text{-}\sigma:\eta^2\text{-}C(CH_3)=CHCH_3\}(\mu\text{-}PMe_2)(CO)_3]$ and $[Cp_2Mo_2\{\mu\text{-}\sigma:\eta^2\text{-}C(CH_3)=CHCH_3\}(\mu\text{-}SR)(CO)_2]$, contain three and two carbonyl groups respectively. Evidently, the electronic properties of the phosphido bridge inhibit decarbonylation of $[Cp_2Mo_2\{\mu\text{-}\sigma:\eta^2\text{-}C(CH_3)=CHCH_3\}(\mu\text{-}PMe_2)(CO)_3]$ whereas the analogous thiolato-bridged species undergoes loss of CO.

Two closely related intermediates can be postulated to explain the formation of the dicarbonyl thiolate compounds **5** and **6**. The first (Scheme 1, path A) contains a $\mu\text{-}\sigma:\eta^2$-vinyl ligand and is the thiolate analogue of the tricarbonyl phosphido-bridged complex $[Cp_2Mo_2\{\mu\text{-}\sigma:\eta^2\text{-}C(CH_3)=CHCH_3\}(\mu\text{-}PMe_2)(CO)_3]$. Its photo-induced decarbonylation gives **5** and **6**. The second pathway (Scheme 1, path B) involves an intermediate with a terminal vinyl ligand which can coordinate to the second molybdenum atom with loss of CO to give the final product. Partial oxidation of **5** with traces of dioxygen gives the Mo(II)–Mo(IV) complex $[Cp_2Mo_2(O)\{\mu\text{-}\sigma:\eta^2\text{-}C(CH_3)=CHCH_3\}(\mu\text{-}SR)(CO)]$ (**7**). Similar oxo

compounds have been obtained by exposure of molybdenum(II) derivatives $[Cp_2Mo_2(CO)_2(\mu\text{-}X)_2]$ (X = PPh$_2$ [16]) and SR (R = Me or Ph [14]) to atmospheric dioxygen, and as a coproduct in the synthesis of $[Cp_2Mo_2\{\mu\text{-}\sigma : \eta^2\text{-}C(R')=CHR''\}(\mu\text{-}PMe_2)(CO)_3]$ [4a].

2.2. The solid state structure of $[Cp_2Mo_2\{\mu\text{-}\sigma : \eta^2\text{-}C(CH_3)=CHCH_3\}(\mu\text{-}SPh)(CO)_2]$ (6) at $-123°C$

Molecules of **6** (Fig. 1) contain two $(\eta^5\text{-}C_5H_5)Mo(CO)$ units linked by an Mo–Mo bond and bridged by SPh and $\mu\text{-}\sigma : \eta^2\text{-}C(CH_3)=CHCH_3$ groups. The centroids of the cyclopentadienyl rings C(1)–C(5) and C(6)–C(10), namely C(Cp1) and C(Cp2), are nearly colinear with the Mo atoms. Distortion from linearity is barely perceptible at Mo(2) (Mo(1)–Mo(2)–C(Cp2), 175.1°) but is significant at Mo(1) (Mo(2)–Mo(1)–

C(Cp1), 156.4°) so that the cyclopentadienyl rings are only very roughly parallel to one another. The carbonyl ligands are *trans* (C(11)–Mo(1)–Mo(2)–C(12), 171.4(4)°) as are the bridging atoms S(1) and C(21) (S(1)–Mo(1)–Mo(2)–C(21), 162.9(3)°). These bridging units are folded symmetrically away from C(12) so that the C(12)–Mo(2)–Mo(1)–S(1) and –C(21) torsion angles are −97.3(3) and 99.9(4)° respectively. The thiolate phenyl ring also points away from C(12); indeed, S(1)–C(13) and Mo(1)–C(11) nearly eclipse each other when viewed along the S(1)–Mo(1) bond (Table 2, torsion angles). The C(12)–O(2) carbonyl ligand thus has a less hindered environment than C(11)–O(1) and, possibly because of this, it semibridges weakly the metal–metal bond (Mo(1)–Mo(2)–C(12), 73.8(2)°; Mo(1) · · · C(12), 2.798(7) Å).

Table 2
Bond lengths (Å) and angles (°) for **6**

Bond lengths

Mo(1)–S(1)	2.431(2)	Mo(1)–Mo(2)	2.644(1)
Mo(1)–C(1)	2.300(8)	Mo(1)–C(2)	2.339(8)
Mo(1)–C(3)	2.352(8)	Mo(1)–C(4)	2.333(8)
Mo(1)–C(5)	2.309(8)	Mo(1)–C(11)	1.938(7)
Mo(1)–C(20)	2.397(7)	Mo(1)–C(21)	2.359(8)
Mo(2)–S(1)	2.390(2)	Mo(2)–C(12)	1.912(8)
Mo(2)–C(21)	2.121(8)	Mo(2)–C(6)	2.314(8)
Mo(2)–C(7)	2.276(7)	Mo(2)–C(8)	2.302(7)
Mo(2)–C(9)	2.355(7)	Mo(2)–C(10)	2.363(7)
S(1)–C(13)	1.793(6)	O(1)–C(11)	1.160(9)
O(2)–C(12)	1.168(9)	C(19)–C(20)	1.513(13)
C(20)–C(21)	1.384(11)	C(21)–C(22)	1.508(12)

Bond angles

C(Cp1)–Mo(1)–Mo(2)	156.4	C(Cp1)–Mo(1)–S(1)	113.2
C(Cp1)–Mo(1)–C(11)	113.7	C(Cp1)–Mo(1)–C(20)	108.3
C(Cp1)–Mo(1)–C(21)	141.3	C(11)–Mo(1)–C(21)	75.0(3)
C(11)–Mo(1)–C(20)	95.8(3)	C(21)–Mo(1)–C(20)	33.8(3)
C(11)–Mo(1)–S(1)	90.2(2)	C(21)–Mo(1)–S(1)	104.1(2)
C(20)–Mo(1)–S(1)	131.2(2)	C(11)–Mo(1)–Mo(2)	88.4(2)
C(21)–Mo(1)–Mo(2)	49.8(2)	C(20)–Mo(1)–Mo(2)	75.7(2)
S(1)–Mo(1)–Mo(2)	56.0(1)	C(Cp2)–Mo(2)–Mo(1)	175.1
C(Cp2)–Mo(2)–S(1)	124.4	C(Cp2)–Mo(2)–C(12)	110.3
C(Cp2)–Mo(2)–C(21)	118.6	C(12)–Mo(2)–C(21)	89.6(3)
C(12)–Mo(2)–S(1)	87.3(2)	C(21)–Mo(2)–S(1)	113.6(2)
C(12)–Mo(2)–Mo(1)	73.8(2)	C(21)–Mo(2)–Mo(1)	58.1(2)
S(1)–Mo(2)–Mo(1)	57.5(1)	C(13)–S(1)–Mo(2)	114.5(2)
C(13)–S(1)–Mo(1)	111.7(2)	Mo(2)–S(1)–Mo(1)	66.5(1)
O(1)–C(11)–Mo(1)	177.4(6)	O(2)–C(12)–Mo(2)	168.8(6)
C(14)–C(13)–S(1)	117.5(5)	C(18)–C(13)–S(1)	122.8(6)
C(21)–C(20)–C(19)	125.9(8)	C(21)–C(20)–Mo(1)	71.6(4)
C(19)–C(20)–Mo(1)	123.1(6)	C(20)–C(21)–C(22)	117.7(8)
C(20)–C(21)–Mo(2)	123.0(6)	C(22)–C(21)–Mo(2)	119.3(7)
C(20)–C(21)–Mo(1)	74.6(5)	C(22)–C(21)–Mo(1)	126.5(7)
Mo(2)–C(21)–Mo(1)	72.1(2)		

Torsion angles

S(1)–Mo(1)–Mo(2)–C(12)	−97.3(3)	C(11)–Mo(1)–S(1)–C(13)	−20.3(4)
C(11)–Mo(1)–Mo(2)–C(12)	171.4(4)	C(20)–Mo(1)–S(1)–Mo(2)	−9.9(3)
C(21)–Mo(1)–Mo(2)–C(12)	99.9(4)	C(21)–Mo(1)–S(1)–Mo(2)	13.4(3)
S(1)–Mo(1)–Mo(2)–C(21)	162.9(3)	C(19)–C(20)–C(21)–C(22)	5.6(9)

C(Cp1) and C(Cp2) are the centroids of the cyclopentadienyl rings defined by atoms C(1)–C(5) and C(6)–C(10) respectively.
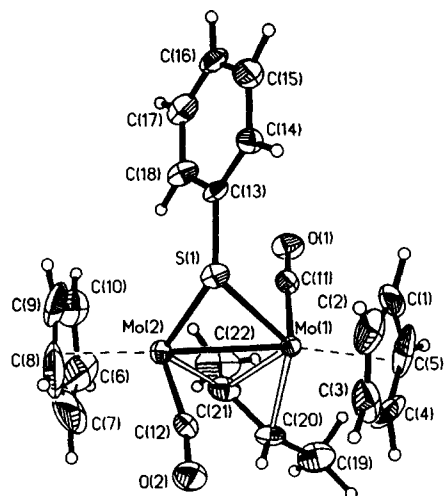
Fig. 1. A view of the molecule of **6** showing the atom-numbering scheme. 50% probability ellipsoids are displayed, except for hydrogen atoms which are represented by spheres of arbitrary radius.

Electron-counting rules require an order of two for the Mo(1)–Mo(2) bond. Its length (2.644(1) Å) is close to the average value of 2.61 Å for 62 such distances obtained from the Cambridge Structural Database [17]. Although there are other examples of structurally characterised complexes containing a simple $\mu\text{-}\sigma:\eta^2\text{-}CR\text{=}CR_2$ bridging two molybdenum atoms, such as $[Cp_2Mo_2\{\mu\text{-}\sigma:\eta^2\text{-}C(CH_3)\text{=}CHCH_3\}(\mu\text{-}PMe_2)(CO)_3]$ [4a], $[Cp_2Mo_2(\mu\text{-}\sigma:\eta^2\text{-}CH\text{=}CH_2)(CO)_4]$ [18] and $[Cp_2Mo_2(\mu\text{-}\sigma:\eta^2\text{-}CH\text{=}CHPh)(CO)_4(H_2O)]^+$ [19], all involve Mo–Mo bonds with orders less than two and Mo–Mo distances greater than 3 Å. In $[Cp_2Mo_2\{\mu\text{-}C(CO_2Me)\text{=}CHCO_2Me\}(\mu\text{-}S^iPr)(CO)_2]$, formally an exact analogue of **6**, the Mo–Mo bond order is reduced to one through coordination of CO_2Me oxygen to one of the metal atoms and the Cp rings appear to be *trans* with respect to the Mo–Mo bond [12], in contrast with the nearly linear Cp–Mo–Mo–Cp arrangement in **6**. Despite the much shorter Mo–Mo bond in **6** the length
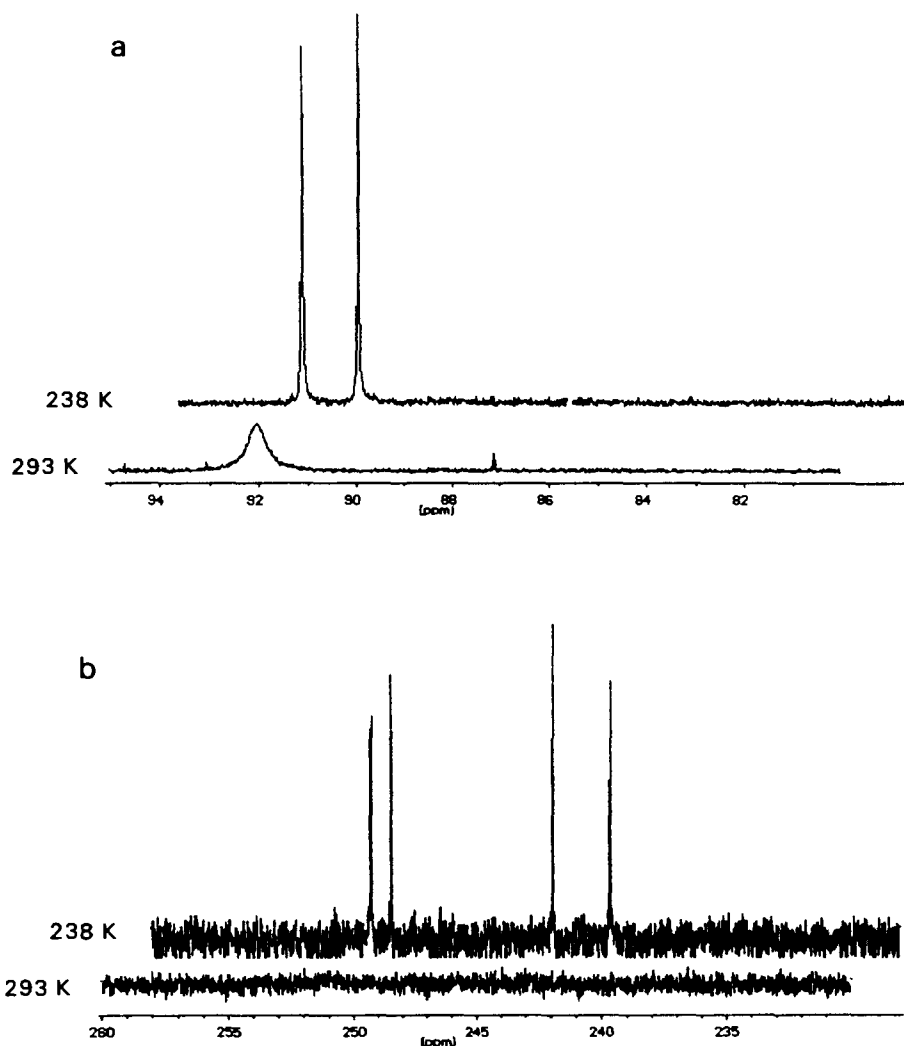

Fig. 2. ^{13}C {^1H} NMR spectra of **9** at 293 and 238 K (CD_3CN): (a) cyclopentadienyl region, (b) carbonyl region.

of the Mo(2)–C(21) σ bond (2.121(8) Å) is comparable with the mean value for the corresponding bond in the μ-phosphido complex (2.089 Å) and the Mo(1)–C(21) and Mo(1)–C(20) π bonds (2.359(8) and 2.397(7) Å) are only slightly longer than those in the phosphido complex (2.321–2.329 Å). The C(19)–C(22) carbon skeleton of the vinyl ligand in 6 is very nearly planar (C(19)–C(20)–C(21)–C(22), 6(1)°) and the methyl groups are cis.

Other distances in 6 are close to expected values [20]. The bridging S(1) atom is slightly closer to Mo(2) than to Mo(1) although the difference between the Mo–S distances (0.041(3) Å) is not great. We note that both Cp rings appear to display appreciably anisotropic thermal motion (Fig. 1) even at −123°C. This may be due to ring libration, although unresolved static disorder of the rings cannot be excluded. It is also worth noting that 6 is asymmetric by virtue, inter alia, of the chiral carbon atom C(21) and that its space group is also chiral. The structure analysis suggests that the crystal used was optically pure, and it follows that all the molecules which composed it had the absolute configuration shown in Fig. 2.

2.3. Deprotonation of the Mo–H bond in [Cp₂Mo₂(μ-H)(μ-SR)(CO)₄] (R = Me (1) or Ph (2))

2.3.1. Reaction with LiBu

In the same way as their phosphido analogues [Cp₂Mo₂(μ-H)(μ-PRR')(CO)₃] (R = R' = Me [21]) (R = Ph; R' = H [7]) and other homodimetallic and heterodimetallic hydrides [3e,22], 1 and 2 are acidic and therefore react readily with bases. Reaction of 1 and 2 with LiBu affords green solutions which have been shown by IR and NMR (¹H and ¹³C) spectroscopy to contain two highly air-sensitive anionic compounds [CpMo(Co)₃]⁻ and [Cp₂Mo₂(μ-SR)(CO)₄]⁻ (R = Me(8) and Ph(9)). Complexes 8 and 9 are easily protonated to regenerate 1 and 2 (Scheme 2).
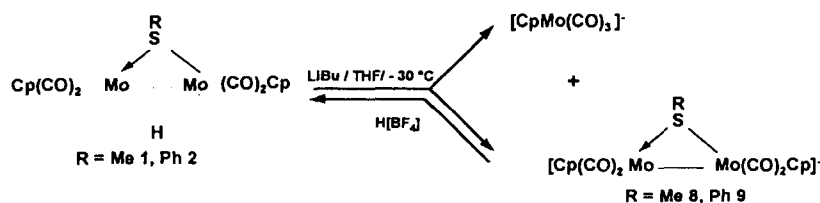
The known mononuclear species [CpMo(CO)₃]⁻ [23] has been identified by comparison of its spectral data with those of an authentic sample. Its formation indicates that there is significant decomposition of 1 and 2

in the presence of base and that under these conditions the thiolate bridge is unable completely to inhibit fragmentation of the dimeric compound.

¹H and ¹³C NMR spectra of [Cp₂Mo₂(μ-SR)(CO)₄]⁻ (Table 3 and Figs. 2 and 3), at room temperature and low temperatures, suggest that fluxional processes are operative in solution. Complexes 8 and 9 were identified principally by NMR spectra recorded at low temperatures. Their ¹H NMR spectra at 213 or 238 K display two inequivalent cyclopentadienyl rings and one SR group. The ¹³C patterns of the CO and cyclopentadienyl consist of four and two signals respectively (Fig. 2). This suggests that at low temperature the Cp and CO groups are trans to the Mo–Mo axis in 8 and 9 (Scheme 3).

2.3.2. Dynamic NMR studies of [Cp₂Mo₂(μ-SR)(CO)₄]⁻ (8 and 9)

The ¹H NMR spectra of 9 between 240 and 291 K are shown in Fig. 3. At 240 K there are two Cp signals of equal intensity at 5.07 and 4.80 ppm. On warming, broadening and coalescence of these Cp signals occur. At 291 K the spectrum shows one broad singlet, at 4.88 ppm. Fast decomposition occurs at higher temperatures (between 291 and 353 K). Similar behaviour was observed for 8. The activation barrier for the observed dynamic process can be estimated from the chemical shift difference Δv and from the coalescence temperature of the Cp signals in the ¹H NMR spectrum ($\Delta G^{\neq}$ = $4.575 T_c(9.972 + \log_{10} T_c - \log_{10} \Delta v)$ [24]). The value of the energy barrier for 9 (SR = SPh) is 56.5 ± 1 kJ mol⁻¹. This is close to that expected for inversion at the sulphur atom [25] but our data (Table 3 and Fig. 3) are not consistent with such a process. Indeed, cis–trans isomerization would imply two signals at low temperatures for the SR groups whereas only one is observed. A trans ↔ trans interconversion involving a trigonal-bipyramidal intermediate is proposed to explain the fluxional process (Scheme 4). This proposal is similar to one used to explain the fluxional behaviour of the heterodimetallic complexes [Mn(CO)₄(μ-P(C₆H₄-p-CH₃)₂Mo(CO)₂Cp]⁻ [22b] and [Fe(CO)₄(μ-As(CH₃)₂Mo(CO)₂Cp] [26], in which square pyrami-

Scheme 2.

Table 3
IR and NMR data of **8** and **9**

Complex	IR [a], δ (cm^{-1})	^{1}H NMR, δ (ppm)		^{13}C NMR [b], δ (ppm)	
		293 K [c]	213 K [d], 238 K [c]	293 K [c]	213 K [d], 238 K [c]
8	1860 (s), 1800 (m)	4.97 (s, 10H, C$_5$H$_5$), 2.20 (s, 3H, S-CH_3)	4.87 (s, 5H, C$_5$H$_5$) [d], 4.86 (s, 5H, C$_5$H$_5$), 2.09 (s, 3H, S-CH_3)	91.55 (C$_5$H$_5$)	250.93, 248.34, 244.34, 241.30 (CO) 91.02, 90.85 (C$_5$H$_5$) 32.83 (S-CH$_3$) [d]
9	1850 (s), 1805 (m)	7.32–6.96 (m, 5H, S-C$_6$H$_5$), 4.88 (s, 10H, C$_5$H$_5$)	7.70–6.96 (m, 5H, S-C$_6$H$_5$) [c], 5.07 (s, 5H, C$_5$H$_5$), 4.80 (s, 5H, C$_5$H$_5$)	151.09, 133.58, 127.70, 125.70 (SC$_6$H$_5$) 92.07, (C$_5$H$_5$)	251.80, 250.47, 243.90, 241.64 (CO) 149.70, 133.25, 127.57, 125.70 (S-C$_6$H$_5$) 92.55, 91.39 (C$_5$H$_5$) [c]

[a] In CH$_2$Cl$_2$ solution.
[b] Hydrogen-1 decoupled.
[c] In CD$_3$CN.
[d] In THF-d_8.

dal enantiomers are interconverted via a trigonal-bipyramidal intermediate. At room temperature, only one resonance is observed for the Cp ligands (A = B = A' = B'). At low temperatures the two isomers do not interconvert, and the NMR spectra exhibit two peaks for Cp rings ((A = A') ≠ (B = B')) and four in the carbonyl region ((a = a') ≠ (b = b') ≠ (c = c') ≠ (d = d')) (Scheme 4).

2.4. Reductive electrochemistry of [Cp$_2$Mo$_2$(μ-H)(μ-ER)(CO)$_4$] (R = SMe (1), SPh(2), S^{t}Bu (3) and SePh (4))

2.4.1. The primary reduction.

The cyclic voltammogram of [Cp$_2$Mo$_2$(μ-H)(μ-SMe)(CO)$_4$] (**1**) in a CH$_3$CN–[Bu$_4$N][PF$_6$] electrolyte displays one reduction step (Fig. 4(a)), together with oxidation steps which we will not discuss here. The potential of the primary reduction for **1–4** (Table 4) is little affected by the nature of the chalcogen substituent (ER) although the reversibity of this step depends on the nature of the bridge. It is irreversible for **2–4** (ER =
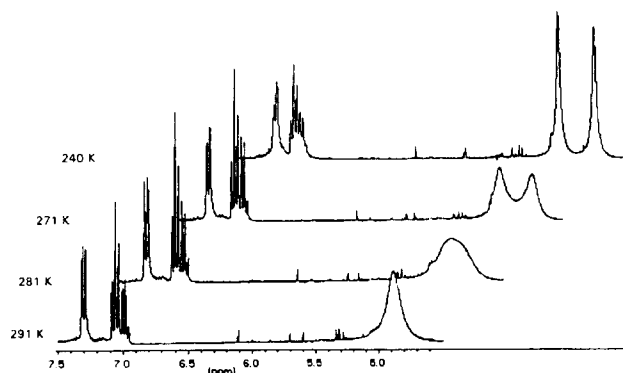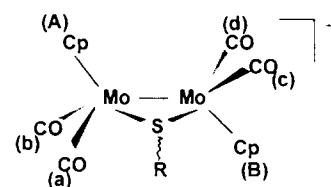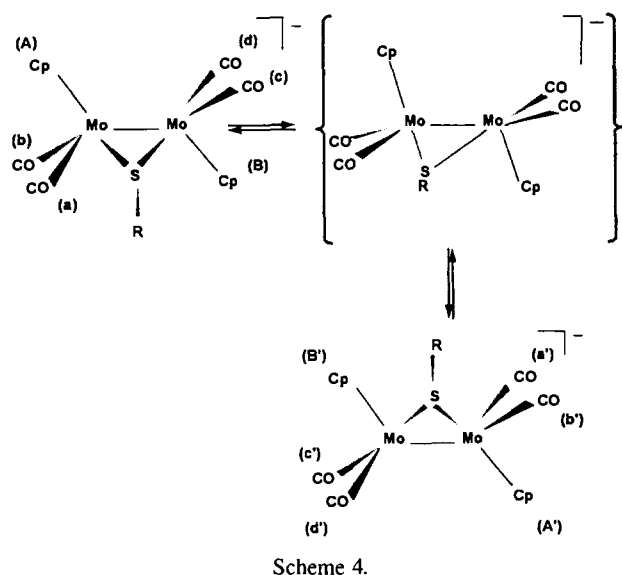
S^{t}Bu, SPh or SePh) though the electrochemical reversibility is greater for **1** (ER = SMe). When the cyclic voltammetry of **1** is run at low temperatures (Fig. 4(b)) ($T = 233$ K) the peak separation between $(E^a_p)_{red1}$ and $(E^c_p)_{red1}$ increases and, if the scan is reversed after $(E^c_p)_{red1}$, a more reversible system appears at -1.83 V [27]. These observations suggest that the reduction of **1** occurs by an ECE-type mechanism [27]. Comparison of $(i^c_p)_{red1}$ to $(i_p)_{ox1}$ [28] for **1** shows that the reduction involves the transfer of two electrons. In a tetrahydrofuran (THF)–[Bu$_4$N][PF$_6$] electrolyte at room temperature, the reduction remains irreversible for **2–4** and quasi-reversible for **1** (Fig. 5(a)). Comparison of $(i^c_p)_{red1}$ with $(i_p)_{ox1}$ indicates that this process involves the transfer of two electrons, as in a CH$_3$CN–[Bu$_4$N][PF$_6$] electrolyte.

2.4.2. Electrolysis.

Exhaustive controlled-potential electrolyses carried out at $E_{p_{red1}}$ require 1 F mol^{-1} of starting material of **1–4**. The cyclic voltammograms of the catholytes (green solutions) show an irreversible reduction in the ($-2.8; -3.0$) range and two reversible oxidations at about -0.9 and -0.5 V (Fig. 5(b) and Table 5). The product of the electrolysis has been designated [Cp$_2$Mo$_2$(μ-ER)(CO)$_4$]$^-$ for the following reasons.

Fig. 3. Variable-temperature ^{1}H NMR spectra (in CD$_3$CN) of **9** in the cyclopentadienyl and SPh regions.

Scheme 3.

Scheme 4.

Fig. 4. Cyclic voltammetry of a solution of [$Mo_2Cp_2(CO)_4(\mu$-H)(μ-SMe)] (1) in CH_3CN–[Bu_4N][PF_6] (vitreous carbon electrode; scan rate 0.2 V s^{-1}). (a) at 293 K; (b) at 233 K.

(i) Protonation of the catholyte regenerates the initial compound (90%yield).

(ii) Deprotonation of **1–4** with Et_3N, NaOMe or Bu_4NOH lead to species having the same cyclic voltammogram as the products of the electrolyses.

(iii) The cyclic voltammogram of the complex synthesized from the reaction between [$Cp_2Mo_2(\mu$-H)(μ-SPh)(CO)$_4$] (**2**) and LiBu, and which has been identified by ^{1}H and ^{13}C NMR spectroscopy as [$Cp_2Mo_2(\mu$-SPh)(CO)$_4$]$^-$ (**9**) is the same as that obtained via electrolysis of **2**.

2.4.3. The reduction mechanism of [$Cp_2Mo_2(\mu$-H)(μ-ER)(CO)$_4$].

Since the primary reduction involves the transfer of two electrons, the consumption of 1 F mol^{-1} during the electrolyses indicates that other reactions not detected on the cyclic voltammetry time scale must occur during
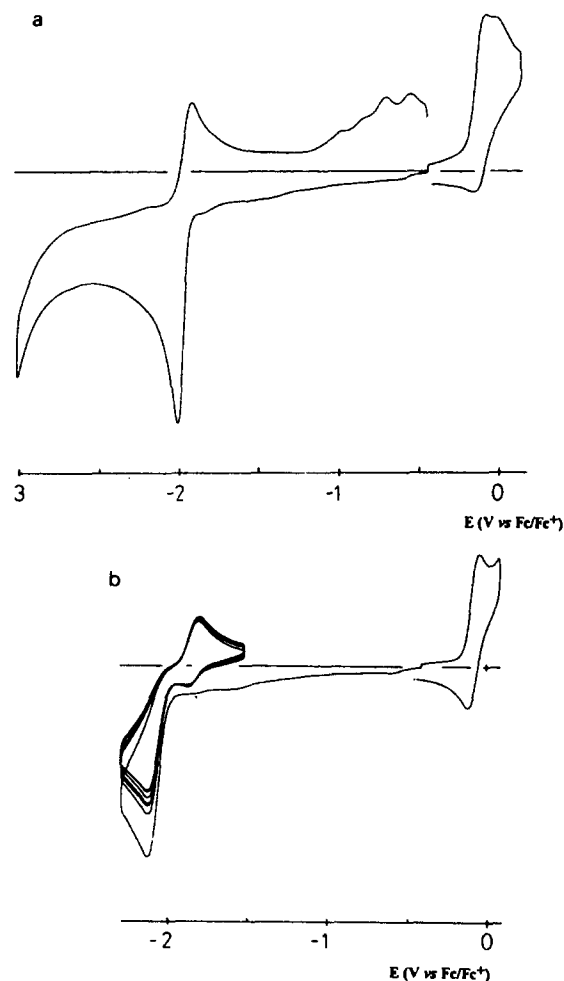
the exhaustive reduction of **1–4**. This reduction arises by an ECE mechanism on the cyclic voltammetry time scale, giving the anionic intermediate [$Cp_2Mo_2(H)(\mu$-

Table 4

Redox potentials of complexes [$Cp_2Mo_2(\mu$-H)(μ-ER)(CO)$_4$] (**1–4**) in nonaqueous media [a]

ER	Solvent	$(E_p)_{red1}$ (V)	$(E^{1/2})_{ox1}$ (V)	$(E_p)_{ox2}$ (V)
SMe (**1**)	MeCN	− 2.03 (− 1.87) [b]	− 0.07	+ 0.10
	THF	− 2.20 (− 2.0) [b]	− 0.01	+ 0.50
SPh (**2**)	MeCN	− 1.92	− 0.06	+ 0.12
	THF	− 2.11	− 0.06	+ 0.11
S^{t}Bu (**3**)	MeCN	− 2.0	− 0.05	+ 0.12
	THF	− 2.21	− 0.07	+ 0.10
SePh (**4**)	MeCN	− 1.85	− 0.02	+ 0.12
	THF	− 2.06	+ 0.09(E_p)	—

[a] Cyclic voltammetry at room temperature unless stated otherwise; $v = 0.2$ V s^{-1}.

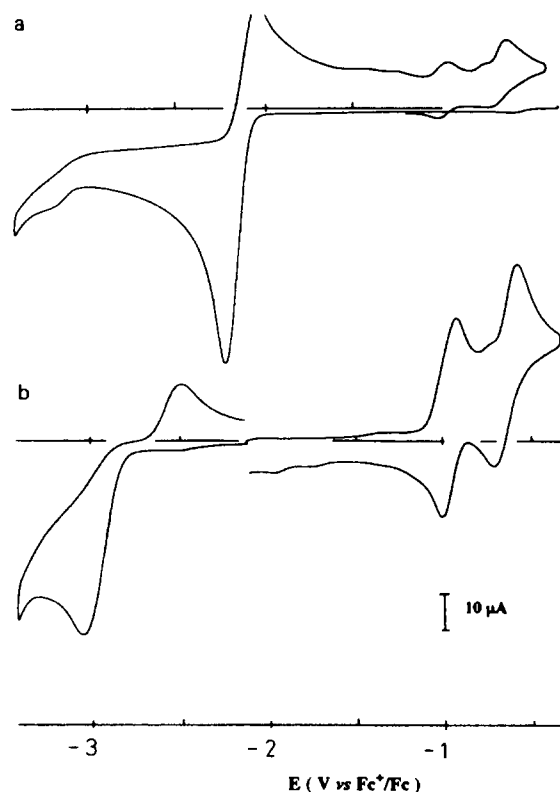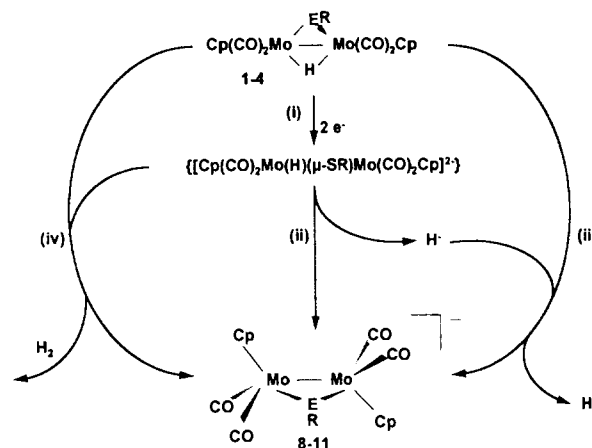[b] The values in parentheses are the potentials of the anodic peak $(E_p^a)_{red1}$.

Fig. 5. Cyclic voltammetry of $[Mo_2Cp_2(CO)_4(\mu-H)(\mu-SMe)]$ (1) in THF–$[Bu_4N]$ $[PF_6]$ (vitreous carbon electrode; scan rate, 0.2 V s^{-1}). (a) before electrolysis; (b) after reduction at -2.4 V (1 F mol^{-1} complex).

Table 5
Redox potentials of complexes $[Mo_2Cp_2(CO)_4(\mu-ER)]^-$ (8–11) in THF–$\{Bu_4N\}[PF_6]$

ER	$(E_p)_{red}$ (V)	$(E^{1/2})_{ox1}$ (V)	$(E_p)_{ox2}$ (V)
SMe (8)	-3.00	-0.94	-0.63
SPh (9)	-2.89	-0.92	-0.59
S^{t}Bu (10)	-3.01	-1.00	-0.55
SePh (11)	-2.80	-0.91	-0.55

Scheme 5.

$ER)(CO)_4]^{2-}$ (Scheme 5, reaction (i)). Its nature cannot be ascertained, but the formulation requires the disruption of the hydride bridge and of the metal–metal bond. Two mechanisms can explain the consumption of 1 F mol^{-1} during the electrolyses. The first proceeds via the loss of the hydride ligand to give the products 8–11 (Scheme 5, reaction (ii)). The free hydride can react with the parent complexes 1–4 to generate $[Cp_2Mo_2(\mu-ER)(CO)_4]^-$ (Scheme 5, reaction (iii)). The second mechanism involves the reaction of the dianionic intermediate $[Cp_2Mo_2(H)(\mu-ER)(CO)_4]^{2-}$ with
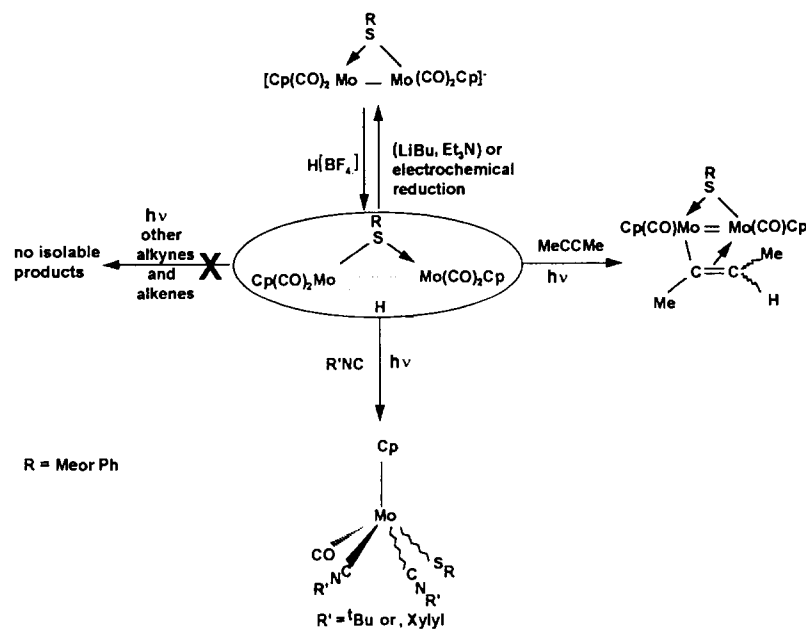
Scheme 6.

$[Cp_2Mo_2(\mu\text{-H})(\mu\text{-ER})(CO)_4]$ which leads to **8–11** with release of H_2 (Scheme 5, reaction (iv)). In both cases, the net charge consumption is 1 F mol^{-1} of starting material.

3. Conclusions

Some aspects of the chemistry of the (hydrido)thiolato-bridged compounds $[Cp_2Mo_2(\mu\text{-H})(\mu\text{-ER})(CO)_4]$ are summarized in Scheme 6. Their reactivity appears rather limited compared with that of their phosphido-bridged analogues [3–5]. This may be ascribed to the greater ability of the phosphido ligand to stabilize polynuclear species. The presence of only one SR bridging group in **1** and **2** is insufficient to inhibit fragmentation and decarbonylation of the dinuclear framework. Effective stabilization of the dimeric species requires more than one thiolate bridge.

4. Experimental section

4.1. General procedures

The reactions were performed under argon using standard Schlenk techniques and solvents were deoxygenated and dried by standard methods.

IR spectra were obtained with a Perkin–Elmer 1430 instrument, and NMR spectra were recorded on a Bruker AC300 spectrophotometer. Peak positions are relative to tetramethylsilane as an internal reference. Mass spectroscopy (MS) was formed out on a Helwett–Packard 5595C gas chromatograph–mall spectrometer. Chemical analyses were performed by the Centre de Microanalyses du CNRS, Vernaison. UV irradiations were performed by using a Hanau TQ 150 mercury vapour lamp placed approximately 10 cm from a Pyrex vessel. Literature methods were used for preparation of $[Cp_2Mo_2(\mu\text{-H})(\mu\text{-ER})(CO)_4]$ [6].

4.2. Reactions of $[Cp_2Mo_2(\mu\text{-H})(\mu\text{-ER})(CO)_4]$ (ER = SMe (1) or SPh(2)) with CH_3CCCH_3

The complex $[Cp_2Mo_2(\mu\text{-H})(\mu\text{-ER})(CO)_4]$ (ER = SMe (**1**) or SPh (**2**)) (300 mg, 0.6 mmol (R = Me) and 0.55 mmol (R = Ph)) was dissolved in toluene (30 ml) and irradiated with UV light for 36 h in the presence of an excess of but-2-yne (1.2–1.9 mmol). The solution changed from red to orange–brown during this time. The solvent was then removed under vacuum and the residue, after being dissolved in the minimum of CH_2Cl_2, was chromatographed on a silica gel column. Elution with hexane: CH_2Cl_2 (3 : 1) gave minor coproducts $[Cp_2Mo_2(CO)_6]$ and $[Cp_2Mo_2(\mu\text{-SR})_2(CO)_2]$ as well as unreacted $[Cp_2Mo_2(\mu\text{-H})(\mu\text{-SR})(CO)_4]$, and an

Table 6
Atomic coordinates and equivalent isotropic displacement parameters for **6**, where U_{eq} is defined as one third of the trace of the orthogonalized U_{ij} tensor

Atom	x ($\times 10^{-4}$)	y ($\times 10^{-4}$)	z ($\times 10^{-4}$)	U_{eq} ($\times 10^{-3}$ Å^2)
Mo(1)	2076(1)	729(1)	3524(1)	18(1)
Mo(2)	4333(1)	1435(1)	2666(1)	30(1)
S(1)	2602(2)	265(1)	2139(1)	25(1)
O(1)	74(7)	2437(4)	2945(3)	39(1)
O(2)	5890(7)	−173(5)	3638(4)	46(2)
C(1)	−106(11)	−149(8)	3698(7)	60(3)
C(2)	1005(13)	−823(6)	3600(5)	51(2)
C(3)	1979(11)	−758(7)	4223(6)	54(3)
C(4)	1500(14)	−53(8)	4733(6)	60(3)
C(5)	186(13)	345(7)	4424(7)	62(3)
C(6)	5880(12)	2766(8)	2456(5)	90(5)
C(7)	6768(9)	1939(10)	2577(7)	127(8)
C(8)	6523(11)	1304(8)	1932(7)	103(6)
C(9)	5482(11)	1739(7)	1413(5)	74(4)
C(10)	5085(9)	2642(6)	1736(5)	66(3)
C(11)	849(8)	1803(5)	3149(4)	27(2)
C(12)	5161(8)	409(6)	3304(4)	31(2)
C(13)	1234(7)	755(5)	1456(4)	23(1)
C(14)	166(9)	121(6)	1147(4)	28(2)
C(15)	−864(11)	430(7)	579(5)	44(2)
C(16)	−827(10)	1398(7)	328(4)	38(2)
C(17)	212(11)	2019(6)	622(5)	38(2)
C(18)	1265(10)	1720(5)	1191(4)	31(2)
C(19)	2846(14)	2077(7)	5237(6)	51(2)
C(20)	3510(9)	1664(6)	4471(5)	30(2)
C(21)	3566(10)	2128(6)	3731(5)	36(2)
C(22)	3042(17)	3170(6)	3692(7)	58(3)

orange band yielding **5** or **6**. Complex **7** was then eluted with CH_2Cl_2 as a purple band. Complexes **5–7** were washed with pentane.

5: brown solid; yield, 40%. Anal. Found: C, 42.0; H, 4.3. $C_{17}H_{20}Mo_2O_2S$ Calc.: C, 42.5; H, 4.2%. MS: m/z 480 (M^+).

6: brown solid; yield, 45%. Anal. Found: C, 48.7; H, 4.3; S, 5.8. $C_{22}H_{22}Mo_2O_2S$ Calc.: C, 48.7; H, 4.1; S, 5.9%. MS: m/z 542 (M^+).

7: purple solid; yield, 5–10%. MS: m/z 468 (M^+).

4.3. Deprotonation of $[Cp_2Mo_2(\mu\text{-}H)(\mu\text{-}ER)(CO)_4]$ (1 and 2)

One equivalent of LiBu was added to a solution of **1** (300 mg, 0.6 mmol) or **2** (300 mg, 0.55 mmol) in THF at $-60°C$. When the temperature reached 25°C, the solution became green. The solvent was then removed under vacuum and the residue was washed twice with 10 ml of pentane. The proportion of $[Cp_2Mo_2(\mu\text{-}SR)(CO)_4]^-[CpMo(CO)_3]^-$, determined from ^1H NMR spectra, varies from 9.5 to 4.

4.4. Crystal structure analysis of $C_{22}H_{22}Mo_2O_2S$ (6)

All measurements were made at $-123°C$ on an Enraf–Nonius CAD4 diffractometer equipped with an Oxford Cryostream Cooler using graphite-monochromated Mo Kα radiation ($\lambda = 0.71073$ Å). The crystal was an orange prism $0.20 \times 0.20 \times 0.10$ mm.

4.4.1. Crystal data

$C_{22}H_{22}Mo_2O_2S$; $M = 542.34$; orthorhombic; space group, $P2_12_12_1$; $a = 8.880(2)$, $b = 13.746(3)$ and $c = 16.605(3)$ Å; $V = 2026.9(7)$ Å^3; $Z = 4$; $D_{calc} = 1.777$ g cm^{-3}; $\mu = 1.355$ mm^{-1}.

4.4.2. Measurements

Cell dimensions are based on the setting angles of 25 reflections with $11 \leqslant \theta$(Mo Kα) $\leqslant 21°$. The intensities of 3336 unique reflections with θ(Mo Kα) $\leqslant 30°$, $0 \leqslant h \leqslant 12$, $0 \leqslant k \leqslant 19$, $-23 \leqslant l \leqslant 0$, were measured from ω–2θ scans. For 2457 of these reflections $I > 2\sigma(I)$. Absorption and extinction corrections were deemed unnecessary.

4.4.3. Structure analysis.

The structure was solved by direct methods [29] and refined using 3330 unique reflections by the full-matrix least-squares method on F^2 with $w = 1/[\sigma^2(F) + a^2P^2 + bP]$ ($a = 0.035$, $b = 2.22$ and $P = (F_{obs} + 2F_{calc})/3$). Refinement of 272 parameters (Table 6) converged $(\Delta/\sigma < 0.18)$ at $R[F, 2\sigma(I)] = 0.037$, $R_w(F^2$, all data) $= 0.102$, $S = 1.09$ with $|\Delta\rho| < 0.98$ electrons Å^{-3}. For non-hydrogen atoms, positional and anisotropic displacement parameters were freely refined

except for the fractional coordinates of the cyclopentadienyl carbon atoms C(6)–C(10) which comprised a variable-metric rigid group [30]. Cp H atoms rode on their parent C atoms with $U(H) = 0.080$ Å^2 (ring C(1)–C(5)) or $1.2U_{eq}(C)$ (ring C(6)–C(10)). For other H atoms, U was fixed at 0.050 Å^2 but the fractional coordinates were refined. The absolute configuration was confirmed by refinement of the Flack [31] parameter to $x = 0.14(9)$. Calculations were performed on a DCS486 computer using SHELXL-93 and local programs [30,32].

5. Supplementary material available

Tables of crystal data, atomic positional and displacement parameters, and a complete geometry listing are available from the Cambridge Crystallographic Data Centre.

References and notes

[1] S. Poder-Guillou, P. Schollhammer, F.Y. Pétillon, J. Talarmin, S.E. Girdwood and K.W. Muir, *J. Organomet. Chem.*, *506* (1996) 321.

[2] (a) M.Y. Darensbourg and C.E. Ash, *Adv. Organomet. Chem.*, *27* (1987) 1; (b) G.G. Hlatky and R.H. Crabtree, *Coord. Chem. Rev.*, *65* (1985) 1; (c) L.M. Venanzi, *Coord. Chem. Rev.*, *43* (1982) 251; (d) D.S. Moore and S.D. Robinson, *Chem. Soc. Rev.*, *12* (1981) 415.

[3] (a) A.D. Horton, A.C. Kemball and M.J. Mays, *J. Chem. Soc., Dalton Trans.*, (1988) 2953; (b) Lj. Manojlovic'-Muir, K.W. Muir, M.C. Jennings, M.J. Mays, G.A. Solan and K.W. Woulfe, *J. Organomet. Chem.*, *491* (1995) 255; (c) J.A. Iggo, M.J. Mays, P.R. Raithby and K. Henrick, *J. Chem. Soc., Dalton Trans.*, (1983) 2021; (d) K. Henrick, M. McPartlin, J.A. Iggo, A.C. Kemball, M.J. Mays and P.R. Raithby, *J. Chem. Soc., Dalton Trans.*, (1987) 2669; (e) J.A. Iggo, M.J. Mays, P.R. Raithby and K. Henrick, *J. Chem. Soc., Dalton Trans.*, (1984) 633.

[4] (a) G. Conole, K. Henrick, M. Mc Partlin, A.D. Horton and M.J. Mays, *New J. Chem.*, *12* (1988) 559; (b) K. Henrick, M. Mc Partlin, A.D. Horton and M.J. Mays, *J. Chem. Soc., Chem. Commun.*, (1988) 1083.

[5] (a) A.D. Horton, M.J. Mays and P.R. Raithby, *J. Chem. Soc., Chem. Commun.*, (1985) 247; (b) T. Adatia, K. Henrick, A.D. Horton, M.J. Mays and M. McPartlin, *J. Chem. Soc., Chem. Commun.*, (1986) 1206; (c) A.D. Horton, M.J. Mays and P.R. Raithby, *J. Chem. Soc., Dalton Trans.*, (1987) 1557; (d) D.W. Prest, M.J. Mays and P.R. Raithby, *J. Chem. Soc., Dalton Trans.*, (1982) 2021.

[6] P. Schollhammer, F.Y. Pétillon, R. Pichon, S. Poder-Guillou, J. Talarmin, K.W. Muir and S.E. Girdwood, *J. Organomet. Chem.*, *486* (1995) 183.

[7] S. Woodward and M.D. Curtis, J. Organomet. Chem., 439 (1992) 319.

[8] S. Otsuka and A. Nakamura, Adv. Organomet. Chem., 14 (1976) 245.

[9] G.E. Herberich and W. Barlage, Organometallics, 6 (1984) 1924.

[10] S.A. MacLaughlin, S. Doherty, N.J. Taylor and A.J. Carty, Organometallics, 11 (1992) 4315.

[11] A.A.H. van der Zeijden, H.W. Bosh and H. Berke, Organometallics, 11 (1992) 563.

[12] H. Adams, N.A. Bailey, S.R. Gay, T. Hamilton and M.J. Morris, J. Organomet. Chem., 493 (1995) C25.

[13] D. Seyferth, C.M. Archer, D.P. Ruschke, M. Cowie and R.W. Hilts, Organometallics, 10 (1991) 3363.

[14] P. Schollhammer and F.Y. Pétillon, unpublished results.

[15] L.C. Dermott, K.W. Muir, F.Y. Pétillon, S. Poder-Guillou and P. Schollhammer, Acta Crystallogr., in press.

[16] T. Adatia, M. McPartlin, M.J. Mays, M.J. Morris and P.R. Raithby, J. Chem. Soc., Dalton Trans., (1989) 1555.

[17] F.H. Allen, S. Bellard, M.D. Brice, B.A. Cartwright, A. Double-day, H. Higgs, T. Hummelink, B.G. Hummelink-Peters, O. Kennard, W.D.S. Motherwell, J.R. Rodgers, and D.G. Watson, Acta Crystallogr., Sect. B 35 (1979) 2331.

[18] U. Kern, C.G. Kreiter, S. Muller-Becker and W. Frank, J. Organomet. Chem., 444 (1993) C31.

[19] R.F. Gerlach, D.N. Duffy and M.D. Curtis, Organometallics, 2 (1983) 1172.

[20] A.G. Orpen, L. Brammer, F.H. Allen, O. Kennard, D.G. Watson and R. Taylor, International Tables for Crystallography, Vol. C, International Union of Crystallography, Chester, 1992.

[21] J.L. Petersen and R.D. Stewart, Jr., Inorg. Chem., 19 (1980) 186.

[22] (a) J. Boothman and G. Hogarth, J. Organomet. Chem., 437 (1992) 201; (b) C.P. Casey and R.M. Bullock, Organometallics, 3 (1984) 1100.

[23] (a) U. Behrens and E. Edelmann, J. Organomet. Chem., 263 (1984) 179; (b) E.C. Alyea, A. Malek and J. Malito, Polyhe-dron, 5 (1986) 403.

[24] H.S. Gutowsky and C.H. Holm, J. Chem. Phys., 25 (1956) 1228.

[25] (a) S.D. Killops and S.A.R. Knox, J. Chem. Soc., Dalton Trans., (1978) 1260; (b) I.B. Benson, S.A.R. Knox, P.J. Naish and A.J. Welsh, J. Chem. Soc., Dalton Trans., (1981) 2235; (c) Q. Feng, M. Ferrer, M.L.H. Green, P. Mountford, V.S.B. Mtetwa and K. Prout, J. Chem. Soc., Dalton Trans., (1991) 1397.

[26] C.P. Casey and R.M. Bullock, J. Organomet. Chem., 218 (1981) C47.

[27] i_p^a is the anodic peak current, i_p^c is the cathodic peak current, E_p is the peak potential, $E^{1/2} = (E_{pa} + E_{pc})/2$, $\Delta E = E_{pa} - E_{pc}$, v is the scan rate and n is the number of electrons. An ECE process involves sequential electron transfer (E), chemical (C) and electron transfer (E) steps.

[28] Although the oxidation of the complex was not investigated in detail, the anodic step appears in Figs. 4 and 5 and in Tables 4 and 5.

[29] G.M. Sheldrick, SHELX86, Program for the Solution of Crystal Structures, University of Göttingen, Göttingen, 1986.

[30] G.M. Sheldrick, SHELXL93, Program for the Refinement of Crystal Structures, University of Göttingen, Göttingen, 1993.

[31] (a) H.D. Flack, Acta Crystallogr., Sect. A, 39 (1983) 876; (b) G. Bernardinelli and H.D. Flack, Acta Crystallogr., Sect. A, 41 (1985) 500.

[32] P.R. Mallinson and K.W. Muir, J. Appl. Crystallogr., 18 (1985) 51.